Magnetoexcitons and correlated electrons in quantum dots in a magnetic field

Pawel Hawrylak, Arkadiusz Wojs,* and José A. Brum†
Institute for Microstructural Sciences, National Research Council of Canada, Ottawa, Ontario, Canada K1A 0R6
(Received 6 November 1995; revised manuscript received 12 July 1996)

Magnetoexcitons interacting with strongly correlated electronic states in quantum dots in a strong magnetic field are studied. Exact calculations relate the absorption and emission of few-electron artificial atoms to magnetic-field-induced phase transitions between ''magic'' states. For large compact droplets, the coupling of magnetoexcitons to low-energy excitations (edge magnetorotons) leads to a strong enhancement of the oscillator strength at the Fermi level (Fermi edge singularity) both in absorption and in emission on acceptors. The condensation of edge magnetorotons signals the reconstruction of the droplet and is accompanied by different structures in the absorption spectrum. [S0163-1829(96)03040-8]

I. INTRODUCTION

Electrons in quasi-two-dimensional semiconductor quantum dots[1] form artificial atoms. These atoms interact with elementary excitations of the semiconductor, such as excitons. We investigate here the interaction of excitons with electrons in quantum dots. Excitons can become a useful probe of electronic states in artificial atoms, particularly in high-quality self-assembled dots.[2] In these dots both electrons and holes are confined and charging with free carriers[3] can be achieved without introducing unnecessary and large potential fluctuations, inherent in modulation doped quantum dots. A detailed account of the interaction of an artificial hydrogen atom and an exciton, including the effect of the magnetic field and the polarization of light, has already been given.[4] Here we extend these calculations to excitons in *many-electron* artificial atoms in a magnetic field. We give a detailed account of an exciton in a few-electron ($N=3$) artificial atom. This atom undergoes a series of magnetic-field-induced phase transitions between different angular momentum states, recently observed[5,6] via single-electron capacitance spectroscopy. For large quantum dots we concentrate on excitons as a probe of edge reconstruction of compact[7–9] spin-polarized dots and hence edge states of two-dimensional electron systems in the integer quantum Hall effect regime. Stable compact droplets[7–9] are formed for densities and magnetic-field ranges corresponding to the spin-polarized filled lowest Landau level of a bulk sample (filling factor $\nu=1$). In compact droplets electrons occupy all successive lowest angular momenta states, forming a compact uniform density droplet. The droplets are a simple realization of a chiral Luttinger liquid.[7,10] By varying a magnetic field one can drastically increase the role of Coulomb interactions. This drives the droplet of a chiral Luttinger liquid[7,8] through a series of transitions that can be interpreted as a reconstruction of the droplet edges. The reconstruction corresponds to a breakup of a uniform charge density of the droplet. This complex behavior is due to the competition of the electron-electron interactions, Zeeman, and kinetic energy.[5,6,11,12] The competing interactions, tunable by the applied magnetic field,[6,8,11,12] lead to a series of incompressible ground states with ''magic angular momentum'' values. The dot reconstruction is synonymous with ''magic angular momentum'' transitions in few electron artificial atoms.

We show that, in analogy with the optical study of the integer and fractional quantum Hall effect,[13] optical probes, namely, absorption and emission, can be used to study directly incompressible ''magic'' states in few-electron atoms and edge reconstruction in large dots. A basic picture is developed for the chiral Luttinger liquid that sheds light on otherwise inaccessible problems, e.g., the Fermi edge singularity[14] in an interacting electron system involving a mobile valence hole. The differences between the electron and the hole spectral functions of a compact droplet are discussed and related to the creation of a mobile exciton and to the acceptor related recombination spectrum.[15] The effects of spin and polarization of light are also discussed.

II. MODEL

We start by considering the two-dimensional quantum dot,[6] containing N electrons confined by an effective parabolic potential, with a characteristic energy ω_N. A magnetic field B is applied normal to the plane of the dot. The single-particle Hamiltonian corresponds to a particle moving in a parabolic potential and in the presence of the magnetic field. It can be exactly diagonalized,[6,15] with single-particle energies $E_{mn}=\Omega_+(n+\frac{1}{2})+\Omega_-(m+\frac{1}{2})$ and eigenstates $|m,n;\sigma\rangle$ of two harmonic oscillators and electron spin σ. The frequencies are $\Omega_\pm=[\Omega\pm\omega_c]/2$ ($\hbar=1$ for the rest of this work). The ω_c is the cyclotron energy, $l_0=1/(m^*\omega_c)^{1/2}$ is the magnetic length, m^* is the effective mass, and $\Omega=\sqrt{\omega_c^2+4\omega_0^2}$. The kinetic energy $\sim\Omega_-$ decreases with the magnetic field, while the Coulomb energy increases with the magnetic field. The Coulomb energy is measured in units of exchange energy $E_0=\mathrm{Ry}\sqrt{2\pi}a_0/l_{\mathrm{eff}}$, where Ry is the effective Rydberg, a_0 is the effective Bohr radius, and $l_{\mathrm{eff}}=l_0/(1+4\omega_0^2/\omega_c^2)^{1/4}$ is the effective magnetic length. The same applies to valence-band holes photoexcited in a quantum dot. The valence-band holes are characterized by characteristic frequencies $\Omega_\pm^h=\beta\Omega_\pm$ and energies $E_{mn}^h=-[\Omega_+^h(n+\frac{1}{2})+\Omega_-^h(m+\frac{1}{2})]$ (with the semiconductor gap E_G set to zero). Since holes have the opposite charge to electrons, the angular momentum of holes is opposite to the angular momentum of electrons.

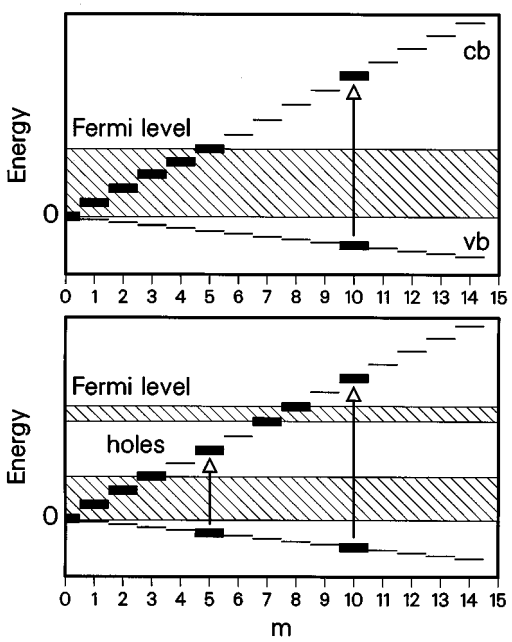

FIG. 1. Schematic picture of single-particle energies E_m for electrons (cb) and valence holes (vb) in the dot as a function of angular momentum m. Vertical arrows indicate possible optical transitions. Upper frame, compact dot; lower frame, reconstructed dot.

If a layer of acceptors is introduced at a distance d from the plane of the dot, photoexcited valence holes localize on negatively charged acceptors.[15,16,17,18] The acceptor complex is charge neutral and a very weak perturbation of the electron system. In the recombination process an electron from the quantum dot recombines with the valence hole leaving a negatively charged acceptor and a ''hole'' in the electron droplet.[17]

In a sufficiently strong magnetic field we restrict the Hilbert space to spin-polarized single-particle states $|m\rangle \equiv |m,0;\downarrow\rangle$ originating from the lowest Landau level.[7,8] As an illustration, the single-particle spectra of seven electrons and a single valence-band hole are shown in Fig. 1, where the electron energies E_m and hole energies E_m^h are shown for $\Omega_-^h = 0.2\Omega_-$. The linear dispersion and the presence of a single branch of excitations resembles a chiral Luttinger liquid.

The dashed areas correspond to occupied electron states and the vertical arrows indicate allowed interband optical transitions. In the case of a compact seven-electron droplet [Fig. 1(a)] these transitions (due to phase-space blocking) are possible only outside the physical area of the dot or, alternatively, into states higher than the Fermi level. The electronic part of this transition can be viewed as an *edge excitation* of a compact $(N+1)$-electron droplet, i.e., with the seventh electron removed from the $m=6$ state and promoted to the $m=10$ state.

A very simplified picture of a reconstructed dot is shown in Fig. 1(b). The reconstruction corresponds to the introduction of holes (unoccupied states) into the bulk of the dot. Correspondingly, one expects a new absorption line to appear in a reconstructed dot as indicated in the figure. This simple picture becomes of course much more complicated due to electron correlations.

After denoting the creation (annihilation) operators for electrons (holes) in states $|m>$ by $c_m^\dagger$ (c_m) and $h_m^\dagger$ (h_m) the Hamiltonian can be written as

$$H = \sum_m E_m c_m^\dagger c_m + E_m^h h_m^\dagger h_m + \frac{1}{2} \sum_{m_1,m_2,m_3,m_4} \langle m_1,m_2|V_{ee}|m_3,m_4\rangle c_{m_1}^\dagger c_{m_2}^\dagger c_{m_3} c_{m_4} + \sum_{m_1,s_2,s_3,m_4} \langle m_1,s_2|V_{eh}|s_3,m_4\rangle c_{m_1}^\dagger c_{m_4} h_{s_2}^\dagger h_{s_3}, \quad (1)$$

where $\langle m_1,m_2|V_{ee}|m_3,m_4\rangle$ are the electron-electron Coulomb matrix elements[7,8] and $\langle m_1,s_2|V_{eh}|s_3,m_4\rangle$ are electron-hole Coulomb matrix elements.[4] The conservation of angular momentum in the Coulomb scattering of electrons guarantees that $m_1+m_2=m_3+m_4$ and for electrons scattered by valence holes $m_1-s_2=m_4-s_3$. While it is possible to compute the electron-hole scattering matrix elements, we relate them to the electron-electron matrix elements as $\langle m_1,s_2|V_{eh}|s_3,m_4\rangle = -\alpha\langle m_1,s_3|V_{ee}|s_2,m_4\rangle$, where $\alpha = |V_{eh}|/V_{ee}$ measures the ratio of the electron-hole to electron-electron interaction. The parameter α can be tuned by, e.g., an electric field applied perpendicular to the plane of the dot.

III. ELECTRONIC STATES

Let us first discuss the $(N+1)$-electron system for a maximally polarized spin configuration $S_z=(N+1)/2$ and an electron system with one spin-flip excitation $S_z=(N-1)/2$, from the point of view of charge and spin excitations. These are the final electronic states after the injection of an exciton.

A. Charge excitations

The total angular momentum $R=\Sigma_i m_i$ of the electron system is a good quantum number and we can label our many electron states by R. For $N+1$ electrons the compact droplet is formed by electrons filling up all lowest angular momentum states $|G_{N+1}\rangle = \Pi_{m=0}^N c_m^\dagger |0\rangle$, with the angular momentum $R_0^{N+1} = N(N+1)/2$. There is only one state with this total angular momentum R_0^{N+1} and hence it is an exact many-electron state. Following earlier bosonization schemes,[7,19] we form the many-electron states $|M,p\rangle$ with total angular momentum $R=R_0^{N+1}+M$ by creating one-pair $|l_1k_1\rangle = c_{l_1}^\dagger c_{k_1}|G_{N+1}\rangle$ and two-pair $|l_2l_1k_2k_1\rangle = c_{l_2}^\dagger c_{l_1}^\dagger c_{k_2} c_{k_1}|G_{N+1}\rangle$ excitations out of the ground state $|G_{N+1}\rangle$:

$$|M,p\rangle=\sum_{\substack{l_1,k_1\\ l_1-k_1=M}} A^{M,p}_{l_1k_1}|l_1k_1\rangle + \sum_{\substack{l_2>l_1,k_2>k_1\\ l_2+l_1-k_2-k_1=M}} B^{M,p}_{l_2l_1k_2k_1}|l_2l_1k_2k_1\rangle. \quad (2)$$

Here $l_i>N$ labels excited states above the last filled state at $m=N$ and $k_i\leqslant N$ labels holes in the compact ground state. The excitation spectra of the $(N+1)$-electron system with a compact ground state $|G_{N+1}\rangle$ are obtained by diagonalizing the electron-electron Hamiltonian in the space of one- and two-pair excitations. They are exact up to $M=9$, where the first three-pair excitation occurs. The matrix elements of the electron-electron Coulomb interaction are given by the following

(a) First are one-pair–one-pair matrix elements, which define a collective excitation spectrum of magnetorotons

$$\langle k_1'l_1'|V_{ee}|l_1k_1\rangle=\delta_{l_1'l_1}\delta_{k_1'k_1}\{\Sigma^{\rm HF}_{l_1}-\Sigma^{\rm HF}_{k_1}\}-\langle l_1'k_1|V_{ee}|k_1'l_1\rangle + \langle l_1'k_1|V_{ee}|l_1k_1'\rangle, \quad (3)$$

with the Hartree-Fock self-energy $\Sigma^{\rm HF}_l=\Sigma_m\langle lm|V_{ee}|ml\rangle - \langle lm|V_{ee}|lm\rangle$. The diagonal part of the scattering matrix element describes a difference of Hartree-Fock self-energies of an electron at $m=l_1$ above the Fermi level and a hole at $m=k_1$ inside the compact dot. The off-diagonal element describes a difference between a *repulsive exchange* and *attractive direct* scattering.

(b) Then there are two-pair–two-pair matrix elements, which define the spectrum of magnetoroton pairs, including possible bound states:

$$\begin{aligned}\langle k_1'k_2'l_1'l_2'|V^{ee}_C|l_2l_1k_2k_1\rangle=&\,\delta_{l_2'l_2}\delta_{l_1'l_1}\delta_{k_2'k_2}\delta_{k_1'k_1}\{\Sigma^{\rm HF}_{l_2}+\Sigma^{\rm HF}_{l_1}-\Sigma^{\rm HF}_{k_2}-\Sigma^{\rm HF}_{k_1}\}+\{\delta_{k_1'k_1}\delta_{k_2'k_2}-\delta_{k_1'k_2}\delta_{k_2'k_1}\}\{-\langle l_2'l_1'|V_{ee}|l_2l_1\rangle\\ &+\langle l_2'l_1'|V_{ee}|l_1l_2\rangle\}+\{\delta_{l_1'l_1}\delta_{l_2'l_2}-\delta_{l_1'l_2}\delta_{l_2'l_1}\}\{\langle k_1k_2|V_{ee}|k_2'k_1'\rangle-\langle k_1k_2|V_{ee}|k_1'k_2'\rangle\}+\delta_{l_1'l_1}\delta_{k_1'k_1}\\ &\times\{-\langle l_2'k_2|V_{ee}|k_2'l_2\rangle+\langle l_2'k_2|V_{ee}|l_2k_2'\rangle\}+\delta_{l_1'l_1}\delta_{k_1'k_2}\{+\langle l_2'k_1|V_{ee}|k_2'l_2\rangle-\langle l_2'k_1|V_{ee}|l_2k_2'\rangle\}\\ &+\delta_{l_1'l_1}\delta_{k_1'k_2}\{+\langle l_2'k_1|V_{ee}|k_2'l_2\rangle-\langle l_2'k_1|V_{ee}|l_2k_2'\rangle\}+\delta_{l_1'l_1}\delta_{k_2'k_2}\{-\langle l_2'k_1|V_{ee}|k_1'l_2\rangle\\ &+\langle l_2'k_1|V_{ee}|l_2k_1'\rangle\}+\delta_{l_1'l_2}\{4\text{terms}\}+\delta_{l_2'l_1}\{4\text{terms}\}+\delta_{l_2'l_2}\{4\text{terms}\}. \end{aligned} \quad (4)$$

This matrix element describes Hartree-Fock energies of two electron-hole pairs and direct and exchange scattering between them.

(c) Finally, there are one-pair–two-pair matrix elements, which define the decay of magnetoroton pairs into one-pair excitations:

$$\begin{aligned}\langle k_1'l_1'|V^{ee}_C|l_2l_1k_2k_1\rangle=&\,\delta_{k_1'k_1}\{+\langle l_1'k_2|V_{ee}|l_1l_2\rangle\\ &-\langle l_1'k_2|V_{ee}|l_2l_1\rangle\}+\delta_{k_1'k_2}\\ &\times\{-\langle l_1'k_1|V_{ee}|l_1l_2\rangle\\ &+\langle l_1'k_1|V_{ee}|l_2l_1\rangle\}\\ &+\delta_{l_1'l_1}\{+\langle k_2k_1|V_{ee}|k_1'l_2\rangle\\ &-\langle k_1k_2|V_{ee}|k_1'l_2\rangle\}+\delta_{l_1'l_2}\\ &\times\{-\langle k_2k_1|V_{ee}|k_1'l_2\rangle\\ &+\langle k_1k_2|V_{ee}|k_1'l_2\rangle\}. \end{aligned} \quad (5)$$

B. Spin-flip excitations

We now consider a possibility of optically injecting electrons with reversed spin, i.e., the total spin of $N+1$ electrons is now $S_z=(N-1)/2$. The many-body electronic states $|M,p\rangle^U$ with one reversed (up) spin and with total angular momentum $R=R^0_{N+1}+M$ are formed analogously to the previous case of $S_z=(N+1)/2$, as the one-pair $|m_1k_1\rangle=c^\dagger_{m_1\uparrow}c_{k_1\downarrow}|G_{N+1}\rangle$ and two-pair $|m_2l_1k_2k_1\rangle=c^\dagger_{m_2\uparrow}c^\dagger_{l_1\downarrow}c_{k_2\downarrow}c_{k_1\downarrow}|G_{N+1}\rangle$ electron-hole excitations out of the spin-polarized compact ground state $|G_{N+1}\rangle$:

$$|M,p\rangle^U=\sum_{\substack{m_1,k_1\\ m_1-k_1=M}} C^{M,p}_{m_1k_1}|m_1k_1\rangle + \sum_{\substack{m_2,l_1,k_2>k_1\\ m_2+l_1-k_2-k_1=M}} D^{M,p}_{m_2l_1k_2k_1}|m_2l_1k_2k_1\rangle. \quad (6)$$

The one-pair excitation $|m_1k_1\rangle$ is now a spin-flip excitation, while in the two-pair excitation there is one spin-flip and one charge excitation. We have adhered here to our notation, which requires excited spin-down electrons to have angular momenta $l_i>N$, but spin-up electrons are allowed all possible angular momenta m_i. Thus single-electron states originating from the lowest spin-up Landau level $|m,0,\uparrow\rangle$ are also included. Contrary to the spin-polarized case, where due to the Pauli principle we had only excitations with positive M, now the additional branch of excitations with negative M appears, which corresponds to spin-flipped electrons moving *towards the center* of the dot.

The excitation spectrum of the $(N+1)$-electron system with $S_z=(N-1)/2$ is obtained through exact diagonalization

of the total Hamiltonian in the above one- and two-pair excitation basis. The spectrum is hence exact up to $M=6-N$, where the first three-pair excited state appears. While including higher excited states is straightforward, the approximate spectrum obtained with only one- and two-pair excited states is fairly accurate for M even far exceeding $6-N$. Among the eigenstates there are ones belonging to the subspace with total spin $S=(N+1)/2$, with energies different from the corresponding eigenenergies of the spin-polarized system only by the Zeeman shift, and ones belonging to the subspace $S=(N-1)/2$. Below we list the Coulomb matrix elements between the states of our basis: (a) one-pair–one-pair, being a difference in the Hartree-Fock energy of the spin-down electron and the Hartree energy of the spin-flip electron and the term defining the attractive (direct) scattering of the excited spin-flipped electron with the hole left in the compact droplet

$$\langle k_1' m_1' | V_{ee} | m_1 k_1 \rangle = \delta_{m_1' m_1} \delta_{k_1' k_1} \{ \Sigma^H_{m_1} - \Sigma^{HF}_{k_1} \} - \langle m_1' k_1 | V_{ee} | k_1' m_1 \rangle, \tag{7}$$

which defines a spectrum of spin-flip collective excitations; (b) two-pair–two-pair, containing all possible scattering processes for four quasiparticles (two electrons with opposite spins and two holes with parallel spins)

$$\begin{aligned}\langle k_1' k_2' l_1' m_2' | V_{ee} | m_2 l_1 k_2 k_1 \rangle = {} & \delta_{m_2' m_2} \delta_{l_1' l_1} \delta_{k_2' k_2} \delta_{k_1' k_1} \{ \Sigma^H_{m_2} + \Sigma^{\mathrm{HF}}_{l_1} - \Sigma^{\mathrm{HF}}_{k_2} - \Sigma^{\mathrm{HF}}_{k_1} \} + \delta_{k_1' k_1} \delta_{k_2' k_2} \langle m_2' l_1' | V_{ee} | l_1 m_2 \rangle + \delta_{l_1' l_1} \\ & \times \{ - \delta_{k_1' k_1} \langle m_2' k_2 | V_{ee} | k_2' m_2 \rangle + \langle m_2' k_1 | V_{ee} | k_2' m_2 \rangle \delta_{k_1' k_2} + \delta_{k_2' k_1} \langle m_2' k_2 | V_{ee} | k_1' m_2 \rangle \\ & - \langle m_2' k_1 | V_{ee} | k_1' m_2 \rangle \delta_{k_2' k_2} \} + \delta_{m_2' m_2} \{ + \delta_{l_1' l_1} (\langle k_1 k_2 | V_{ee} | k_2' k_1' \rangle - \langle k_1 k_2 | V_{ee} | k_1' k_2' \rangle) \\ & - \delta_{k_1' k_1} (\langle l_1' k_2 | V_{ee} | k_2' l_1 \rangle - \langle l_1' k_2 | V_{ee} | l_1 k_2' \rangle) + \delta_{k_1' k_2} (\langle l_1' k_1 | V_{ee} | k_2' l_1 \rangle - \langle l_1' k_1 | V_{ee} | l_1 k_2' \rangle) \\ & + \delta_{k_2' k_1} (\langle l_1' k_2 | V_{ee} | k_1' l_1 \rangle - \langle l_1' k_2 | V_{ee} | l_1 k_1' \rangle) - \delta_{k_2' k_2} (\langle l_1' k_1 | V_{ee} | k_1' l_1 \rangle - \langle l_1' k_1 | V_{ee} | l_1 k_1' \rangle) \}; \end{aligned} \tag{8}$$

and (c) one-pair–two-pair, describing decay of two-pair excitations into one-pair excitations

$$\begin{aligned}\langle k_1' m_1' | V_{ee} | m_2 l_1 k_2 k_1 \rangle = {} & + \delta_{k_1' k_1} \langle m_1' k_2 | V_{ee} | l_1 m_2 \rangle \\ & - \delta_{k_1' k_2} \langle m_1' k_1 | V_{ee} | l_1 m_2 \rangle \\ & + \delta_{m_1' m_2} \{ \langle k_1 k_2 | V_{ee} | k_1' l_1 \rangle \\ & - \langle k_1 k_2 | V_{ee} | l_1 k_1' \rangle \}. \end{aligned} \tag{9}$$

The Coulomb matrix elements for spin-flip and charge excitations are clearly different from the charge-charge excitations in scattering events involving two excited electrons with opposite spin.

IV. ELECTRONS AND A VALENCE-BAND HOLE

We next consider the eigenstates of electrons in the presence of a single mobile valence-band hole. These eigenstates can be labeled by a total angular momentum $R_{\mathrm{tot}}=R-m_h$. The same total angular momentum corresponds to many electronic angular momenta, i.e., the valence hole potential mixes many electronic subspaces.

In the absorption process, illustrated in Fig. 1, an electron–valence-band–hole pair is added to the ground state $|G_N\rangle$ of the N-electron system without changing its total angular momentum R_0^N, but possibly changing total electron spin. Hence optically active states of the $(N+1)$-electron and one-valence-band–hole system belong to Hilbert spaces with a total angular momentum $R_{\mathrm{tot}}=R_0^N$ and spin $S_z=(N+1)/2$ or $S_z=(N-1)/2$. For light polarization injecting a majority spin electron these states are of the form $h_m^\dagger c_m^\dagger |G_N\rangle |0\rangle h = h_m^+ c_m^\dagger c_N |G_{N+1}\rangle |0\rangle_h$, i.e., they correspond to electron-hole pair excitations of the $(N+1)$-electron system, with $M=m-N$, in the presence of a valence-band hole with angular momentum $-m$. Hence all optically active final states of the electron-valence-hole system can be written as

$$\begin{aligned}|f\rangle &= \sum_{M=0}^{\infty} \sum_p D^f_{M,p} |M,p\rangle |N+M\rangle_h \\ &= \sum_{M=0}^{\infty} \Bigg[\sum_{\substack{l_1,k_1 \\ l_1-k_1=M}} A^f_{l_1 k_1} h^\dagger_{N+M} c^\dagger_{l_1} c_{k_1} |G_{N+1}\rangle |0\rangle_h \\ &\quad + \sum_{\substack{l_1,l_2,k_2,k_1 \\ l_1+l_2-k_2-k_1=M}} B^f_{l_2 l_1 k_2 k_1} h^\dagger_{N+M} c^\dagger_{l_2} c^\dagger_{l_1} c_{k_2} c_{k_1} |G_{N+1}\rangle |0\rangle_h \Bigg]. \end{aligned} \tag{10}$$

The valence-band–hole potential mixes electronic states from different electronic angular momentum subspaces. The problem can now be written in terms of a many-electron Wannier equation

$$\begin{aligned}& [e_{M,p} + E^h_{N+M}] D^f_{M,p} \\ & \quad + \sum_{M',p'} \langle M,p;N+M|V_{eh}|M',p';N+M'\rangle D^f_{M',p'} \\ & = E_f D^f_{M,p}, \end{aligned} \tag{11}$$

where $e_{M,p}$ and $|M,p\rangle$ are exact many-electron energies and eigenstates for a given total spin projection S_z.

The absorption spectrum $A(\omega)$ probing the N electron ground state $|G_N\rangle$ of the initial system can now be written in terms of the excitations of the $(N+1)$-electron compact ground state as

$$A(\omega)=\sum_f \left|\left\langle f\left|\sum_{M=0}^{\infty} h^{\dagger}_{N+M}c^{\dagger}_{N+M}c_N\right|G_{N+1}\right\rangle|0\rangle_h\right|^2 \times\delta[E_f-(\omega-\mu_N)], \tag{12}$$

where $\mu_N=E^{\rm GS}_{N+1}-E^{\rm GS}_N$ is the chemical potential of the N electron droplet and the final-state energies are measured from the ground-state energy of the $(N+1)$-electron system $(E^{\rm GS}_{N+1})$.

In the absence of electron–valence-band–hole interactions, the absorption spectrum $A(\omega)$ is simply a spectral function of the N-electron dot. The spectral function is simply related to the probability of adding an extra electron into a single-particle orbital $|m\rangle$: $A(\omega,m)=\Sigma_f|\langle f|c^{\dagger}_m|G_N\rangle|^2\delta[E_f-E^{\rm GS}_N-\omega]$, i.e., to the imaginary part of the retarded Green's function $G(m,\omega)$ of the dot.

In the emission process, we assume that the system of $N+1$ electrons and one valence-band hole, excited into its set of final states $|f\rangle$ in the absorption process, relaxes to its lowest-energy state prior to the recombination. The relaxation takes place due to interaction with phonons.

Hence we can divide the low-temperature absorption and emission processes into the following phases: (i) we start with an N-electron ground state of angular momentum $R_A=R^N_0$; (ii) in the absorption of a photon γ $(Ne+\gamma\rightarrow Ne+X)$ the system of $N+1$ electrons and one valence-band hole is created with the same angular momentum as R_A; (iii) through the interaction with phonons the system relaxes to its ground state, with a new angular momentum R_E, determined by electron-electron and electron–valence-band–hole interactions; and (iv) the electron-hole pair recombines emitting a photon $(Ne+X\rightarrow Ne+\gamma)$, leaving all possible excited states of the N-electron system with the same angular momentum R_E.

At finite temperature and/or finite excitation power one observes the recombination from states corresponding to all possible values of the total angular momentum, including the total angular momentum value corresponding to $R_A=R^N_0$. In the compact N-electron ground state the exciton can be created only outside the compact droplet (at the Fermi level); however, through scattering with phonons, the valence-band hole moves from the edge of the dot into the center (top of the valence band), lowering its kinetic energy and increasing its Coulomb attraction with electrons. Therefore angular momenta of initial states in absorption (R_A) and emission (R_E) differ.

The emission spectrum from the lowest-energy state of the N-electron and one-exciton system is given by

$$E(\omega)=\sum_f \left|\left\langle f\left|\sum_{m=0}^{\infty} h_m c_m\right|i\right\rangle\right|^2\delta[E_f+\omega-\mu_N-E_i], \tag{13}$$

where again μ_N is the chemical potential, the final-state energies E_f of the N-electron dot are measured from the ground-state energy of the N-electron dot $E^{\rm GS}_N$, and the initial (ground-state) energy of $(N+1)$ electrons and a hole (E_i) is measured from the lowest energy of the $(N+1)$ electron system $E^{\rm GS}_{N+1}$. E_i contains a renormalization of all electron energies due to the introduction of the valence hole.

In the absence of electron–valence-band–hole interactions, the emission spectrum $E(\omega)$ is simply a spectral function of a hole (empty state) in the $(N+1)$-electron dot. The spectral function is related to the probability of creating a hole (removing an electron) in an occupied single-particle orbital $|m\rangle$ of the $N+1$ dot: $E(\omega,m)=\Sigma_f|\langle f|c_m|G_{N+1}\rangle|^2\delta[E_f+\omega-E^{\rm GS}_{N+1}]$, i.e., to the imaginary part of the retarded Greens function $G(m,\omega)$ of the dot. The calculation of the electron–valence-band–hole system requires the matrix elements that describe the scattering of one- and two-pair excitations by the valence hole. For charge excitations we find (a) one-pair–one-pair matrix elements, which define scattering of magnetorotons by a valence hole

$$\langle m'_h|\langle k'_1l'_1|V_{eh}|l_1k_1\rangle|m_h\rangle=\delta_{l'_1l_1}\delta_{k'_1k_1}\delta_{m'_hm_h}\Delta^H_{m_h} +\delta_{k'_1k_1}\langle l'_1m'_h|V_{eh}|m_hl_1\rangle -\delta_{l'_1l_1}\langle k_1m'_h|V_{eh}|m_hk'_1\rangle, \tag{14}$$

where $\Delta^H_{m_h}$ is simply a Hartree energy of the valence hole due to interaction with all electrons; (b) two-pair–two-pair matrix elements, which define scattering of magnetoroton pairs by a valence hole

$$\begin{aligned}\langle m'_h|\langle k'_1k'_2l'_1l'_2|V_{eh}|l_2l_1k_2k_1\rangle|m_h\rangle &=\delta_{l'_2l_2}\delta_{l'_1l_1}\delta_{k'_2k_2}\delta_{k'_1k_1}\delta_{m'_hm_h}\Delta^H_{m_h}+\{\delta_{k'_1k_1}\delta_{k'_2k_2}-\delta_{k'_1k_2}\delta_{k'_2k_1}\}\\ &\times\{+\delta_{l'_1l_1}\langle l'_2m'_h|V_{eh}|m_hl_2\rangle-\delta_{l'_2l_1}\langle l'_1m'^{|V_{eh}|m_hl_2}_h\rangle\\ &-\delta_{l'_1l_2}\langle l'_2m'_h|V_{eh}|m_hl_1\rangle+\delta_{l'_2l_2}\langle l'_1m'_h|V_{eh}|m_hl_1\rangle\}\\ &+\{\delta_{l'_1l_1}\delta_{l'_2l_2}-\delta_{l'_1l_2}\delta_{l'_2l_1}\}\{-\delta_{k'_1k_1}\langle k_2m'_h|V_{eh}|m_hk'_2\rangle\\ &+\delta_{k'_2k_1}\langle k_2m'_h|V_{eh}|m_hk'_1\rangle+\delta_{k'_1k_2}\langle k_1m'_h|V_{eh}|m_hk'_2\rangle\\ &-\delta_{k'_2k_2}\langle k_1m'_h|V_{eh}|m_hk'_1\rangle\};\end{aligned} \tag{15}$$

and (c) one-pair–two-pair matrix elements, which define the decay of bound magnetoroton pairs into one-pair excitations via valence-hole scattering

$$\begin{aligned}\langle m'_h|\langle k'_1l'_1|V_{eh}|l_2l_1k_2k_1\rangle|m_h\rangle &=\delta_{l'_1l_1}\{-\delta_{k'_1k_1}\langle k_2m'_h|V_{eh}|m_hl_2\rangle\\ &+\delta_{k'_1k_2}\langle k_1m'_h|V_{eh}|m_hl_2\rangle\}+\delta_{l'_1l_2}\\ &\times\{+\delta_{k'_1k_1}\langle k_2m'_h|V_{eh}|m_hl_1\rangle-\delta_{k'_1k_2}\langle k_1m'_h|V_{eh}|m_hl_1\rangle\};\end{aligned} \tag{16}$$

For spin-flip excitations the Coulomb matrix elements describing scattering of spin-flip excitations and magnetorotons by the valence hole differ from similar processes involving

only charge excitations, as quasielectrons excited over the edge of the droplet are now distinguishable having opposite spins: (a) one-pair–one-pair,

$$\langle m_h'|\langle k_1'm_1'|V_{eh}|m_1k_1\rangle|m_h\rangle = \delta_{m_1'm_1}\delta_{k_1'k_1}\delta_{m_h'm_h}\Delta^H_{m_h} + \delta_{k_1'k_1}\langle l_1'm_h'|V_{eh}|m_hm_1\rangle - \delta_{m_1'm_1}\langle k_1m_h'|V_{eh}|m_hk_1'\rangle; \tag{17}$$

(b) two-pair–two-pair,

$$\begin{aligned}\langle m_h'|\langle k_1'k_2'l_1'm_2'|V_C^{eh}|m_2l_1k_2k_1\rangle|m_h\rangle &= \delta_{m_2'm_2}\delta_{l_1'l_1}\delta_{k_2'k_2}\delta_{k_1'k_1}\delta_{m_h'mh}\Delta^H_{m_h}+\{\delta_{k_1'k_1}\delta_{k_2'k_2} - \delta_{k_1'k_2}\delta_{k_2'k_1}\}\{\delta_{l_1'l_1}\langle m_2'm_h'|V_{eh}|m_hm_2\rangle \\ &+ \delta_{m_2'm_2}\langle l_1'm_h'|V_{eh}|m_hl_1\rangle\} \\ &+ \delta_{l_1'l_1}\delta_{m_2'm_2}\{-\delta_{k_1'k_1}\langle k_2m_h'|V_{eh}|m_hk_2'\rangle \\ &+ \delta_{k_2'k_1}\langle k_2m_h'|V_{eh}|m_hk_1'\rangle+\delta_{k_1'k_2}\langle k_1m_h'|V_{eh}|m_hk_2'\rangle \\ &- \delta_{k_2'k_2}\langle k_1m_h'|V_{eh}|m_hk_1'\rangle\};\end{aligned} \tag{18}$$

and (c) one-pair–two-pair,

$$\begin{aligned}\langle m_h'|\langle k_1'l_1'|V_C^{eh}|m_2l_1k_2k_1\rangle|m_h\rangle &= \delta_{l_1'm_2}\{\delta_{k_1'k_1}\langle k_2m_h'|V_{eh}|m_hl_1\rangle \\ &- \delta_{k_1'k_2}\langle k_1m_h'|V_{eh}|m_hl_1\rangle\}.\end{aligned} \tag{19}$$

V. RESULTS AND DISCUSSION

A. Excitons and ''magic states'' in artificial atoms

It is useful to analyze a simple example. Below we list states for low angular momenta M for $N=4$ electrons with $m=0,1,2,3$ occupied:

$$M:|l_1k_1\rangle|l_2l_1;k_2k_1\rangle;$$

$$0:|3,3\rangle;$$

$$1:|4,3\rangle;$$

$$2:|5,3\rangle,|4,2\rangle;$$

$$3:|6,3\rangle,|5,2\rangle,|4,1\rangle;$$

$$4:|7,3\rangle,|6,2\rangle,|5,1\rangle,|4,0\rangle|5,4;3,2\rangle;$$

$$5:|8,3\rangle,\ldots|6,4;3,2\rangle,|5,4;3,1\rangle.$$

The two-pair excitations start at $M=4$ and their number quickly exceeds the number of one-pair excitations. The first three-pair excitation occurs at $M=9$. Without electron-electron interactions all excited states corresponding to a given M are degenerate, with energy $M\Omega_-$. The electron-electron interactions remove this degeneracy.

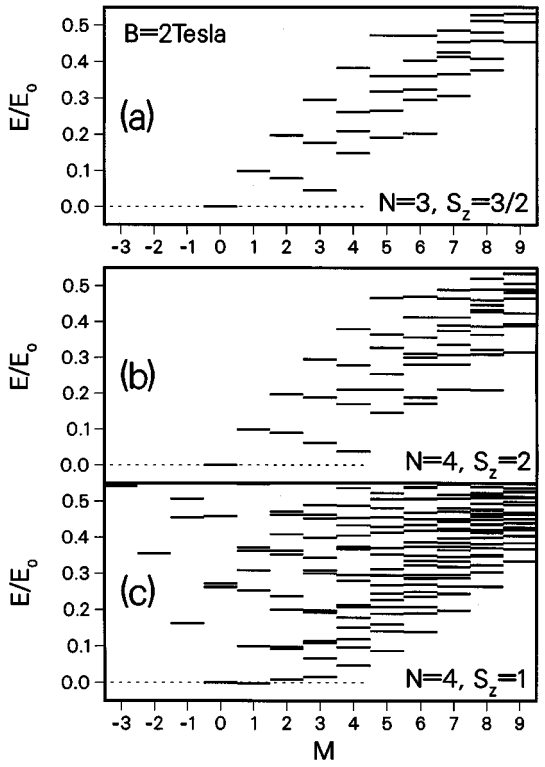

FIG. 2. Electronic excitation energies as a function of excess angular momentum M for $N=3,4$ electrons at a magnetic field $B=2$ T: (a) charge excitations of an $N=3$ compact droplet, (b) charge excitations of an $N=4$ compact droplet, and (c) spin-flip excitations of an $N=4$ compact droplet.

As an illustration, charge and spin-flip excitation spectra of electron droplets with $N=3,4$ electrons in a magnetic field $B=2$ T are shown in Fig. 2 (in all the following figures the parameters taken for computations: effective masses, dielectric constant, etc., are appropriate for GaAs, confining frequency $\omega_N=2.1$ meV both for electrons and holes and $\Omega_-^h=0.2\Omega_-$). These are the initial- and final-state excitation spectra for the absorption process in the $N=3$ electron dot in the absence of electron–valence-band–hole interactions. For spin-polarized systems [Figs. 2(a) and 2(b)] the minima at $M=3$ ($R=6$) for $N=3$ and $M=4$ ($R=10$) for $N=4$ correspond to sets of magic angular momenta, i.e. momenta that will become new ground states at higher values of the magnetic field.[6] In the spin-flip spectrum [Fig. 2(c)] we observe that the ground state has negative energy (measured from the compact spin-polarized state): four electrons with total spin $S=2$ become unstable at this magnetic field.

In Fig. 3 we show the energy spectrum of the exciton interacting with $N=3$ electrons as a function of the total angular momentum for $B=2$ T. We indicate the different subspaces corresponding to absorption ($R_{\rm tot}=R_A$) and emission ($R_{\rm tot}=R_E$).

Figure 4 shows the absorption spectrum of a compact $N=3$ electron dot at $B=2$ T and a reconstructed dot at $B=4$ T. Insets show occupancies $f(m)$ of single-particle states approximately equal to charge density of the dot. The energy of the photon ω includes the zero-point energy $\frac{1}{2}(1+\beta)\Omega$ of the exciton, but the gap E_G between valence and conductance bands has been set to zero. The reconstruc-

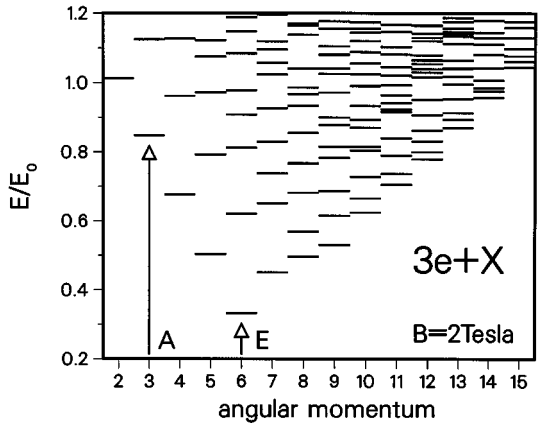

FIG. 3. Excitation spectrum for the system of four electrons and one valence-hole at a magnetic field $B=2$ T. Arrows indicate subspaces with angular momenta $R_A=3$ and $R_E=6$ equal to ground-state angular momenta for initial states in absorption $(3e\rightarrow 3e+X)$ and emission $(3e+X\rightarrow 3e)$, respectively.

tion of the dot corresponds to a transition between magic angular momentum states $R=3$ and $R=6$, observed indirectly in single-electron capacitance measurements.[5,6] For a compact dot the strong lowest-energy peak corresponds to the creation of an exciton at the edge of the droplet [cf. Fig. 7(a)]. For a reconstructed dot the exciton can be injected inside the ring formed by electrons [cf. Fig. 7(c)], minimizing the kinetic energy and increasing the attraction between the hole and electrons. Hence an additional low-energy peak

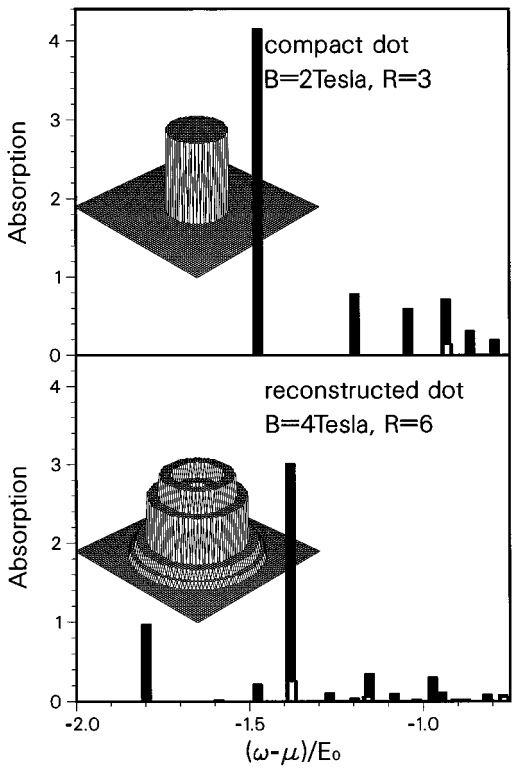

FIG. 4. Absorption spectrum of a compact $N=3$ electron dot at $B=2$ T and a reconstructed dot at $B=4$ T. Insets show occupancies $f(m)=\langle c_m^{\dagger}c_m\rangle$ of single-particle states approximately equal to the charge density of the dot.

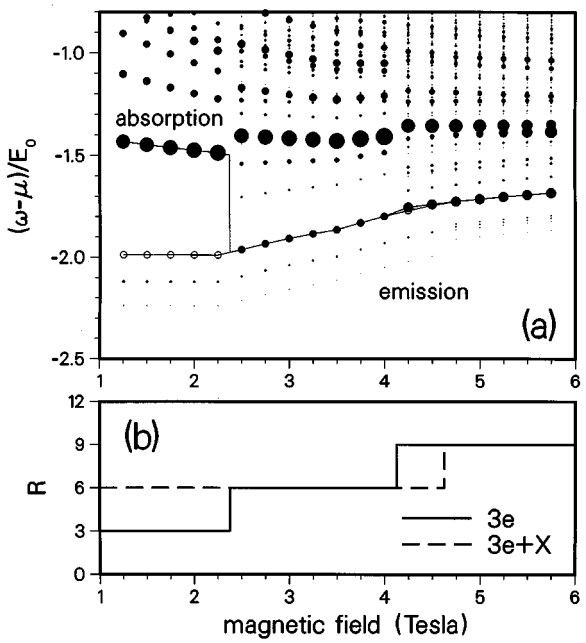

FIG. 5. (a) Evolution of absorption (black dots) and emission (empty dots) spectra for $N=3$ $(3e+X\leftrightarrow 3e)$ with increasing magnetic field. The areas of the dots are proportional to the intensities of the peaks. The solid lines connect lowest-energy peaks in absorption and highest-energy peaks in emission: the separation between them is the absorption-emission shift. (b) Corresponding plot of ground-state angular momenta for the initial states in absorption $(3e)$ and emission $(3e+X)$.

in the absorption spectrum appears as a direct signature of a transition between magic states of the dot.

In Fig. 5(a) the evolution of the absorption and emission spectra as a function of the magnetic field is shown. Figure 5(b) shows the corresponding values of the angular momentum of the $3e$ and the $3e+X$ ground states. The solid lines in Fig. 5(a) connect lowest-energy peaks for absorption and highest-energy peaks for emission. The $B=2$ and 4 T absorption spectra were already shown in Fig. 4. In Fig. 5(a) we can see more clearly that the magnetic-field-induced transitions in the three-electron system (from $R_A=3$ to 6 at $B\approx 2.5$ T and from $R_A=6$ to 9 at $B\approx 4$ T) led to new low-energy lines in the absorption spectrum.

The emission spectra are much simpler than the absorption spectra due to a strongly limited number of final states satisfying conservation of total angular momentum. For magnetic fields up to 4.5 T the initial state of the system has angular momentum $R_E=6$, being almost exactly the product of the four-electron compact state $|G_4\rangle$ and a valence hole occupying the $m=0$ orbital. There are only three possible final states with $R_E=6$, so there are only three peaks in the emission spectrum. Moreover, the highest-energy peak has the largest oscillator strength $\langle f|h_0c_0|i\rangle$ and is most visible. For $B>4.5$ T the initial state undergoes a transition to angular momentum $R_E=9$ and the number of final states increases to 6. However, just like for low magnetic fields, the transition to the compact ground state of the three electrons has much higher intensity than to all others.

The fact that the series of ''magic'' angular momenta for the four-electron and one-hole system is similar to that of three electrons $(R=6,9,12,\ldots)$ corresponds to the fact that

this system can be well approximated as the charge-neutral electron-hole pair (exciton) residing in the center of the dot and surrounded by the ring of three electrons. For higher magnetic fields the three-electron ring expands and the interaction between the exciton and the ring (including exchange between the electron bound to the hole and the surrounding electrons) becomes weak. Hence, with each transition in the initial state to higher angular momentum R_E, the final state can be increasingly well approximated by the product of the three-electron magic ground state for the angular momentum R_E and the ground state of an exciton.

Comparing the spectra in Fig. 5(a) with the discontinuous changes in angular momentum R_A (curve for $3e$) and R_E (curve for $3e+X$) we can observe that for the magnetic fields at which $R_A=R_E$ the edges of absorption and emission spectra coincide. The optical transitions giving the lowest-energy absorption and the highest-energy emission occur between the absolute ground states of the $3e$ and $3e+X$ systems. The Stokes shift between absorption and emission processes is absent.

However, as the discrepancies between R_A and R_E occur, we should see the Stokes shift between absorption and emission, reflecting nonradiative relaxation of the $3e+X$ system. This shift is fairly large for low magnetic fields ($0.5E_0=5$ meV for $B=2$ T), where in the relaxation process the valence-band hole, created at the edge of the compact droplet, moves towards the center of the dot lowering its kinetic energy and increasing attractive interaction with electrons.

The effect of the spin of the photoexcited electron controlled by the polarization of light[4] is illustrated in Fig. 6. Figure 6 shows the evolution of the absorption spectra for spin-polarized and spin-unpolarized cases. While in the case of the spin-polarized state ($S_z=2$) only empty states are allowed for the creation of the exciton, for a spin-flip electron ($S_z=1$) no such restriction holds and the electron-hole pair can freely penetrate the entire area of the dot. This effect is clearly visible when the initial state is compact ($B<2.5$ T). For $S_z=2$ the exciton is created above the Fermi level: for $B=2$ T the peak marked with an open circle *a* corresponds to an exciton created at the edge of the droplet [see Fig. 7(a)]. For $S_z=1$ the low-energy spin-flip exciton can be injected inside the droplet: for $B=2$ T the peak marked as *c* indicates the final state with the hole in the center of the dot surrounded closely by four electrons [see Fig. 7(c)]. Such a configuration minimizes the kinetic energy of the whole system. The resulting difference between energies of first absorption peaks for the two light polarizations is clearly visible in Fig. 6. For $B=2$ T it is $\Delta E=0.44E_0=4.4$ meV. The interaction energies for states marked as *a* and *c* are roughly equal since, for few-electron dots, the increase of the electron-hole attraction for an exciton created in the center and the loss of exchange energy due to flipping of the spin almost cancel each other. Hence the noninteracting picture, where ΔE is just the difference between kinetic energies of an electron-valence hole pair on the $m=0$ orbital and on the Nth orbital; $\Delta E=N(1+\beta)\Omega_-$, offers a fairly good approximation (for $N=3$ and $B=2$ T this is $0.48E_0$). Hence the splitting of absorption lines for two different polarizations provides a good measure of the number of carriers N in the dot.

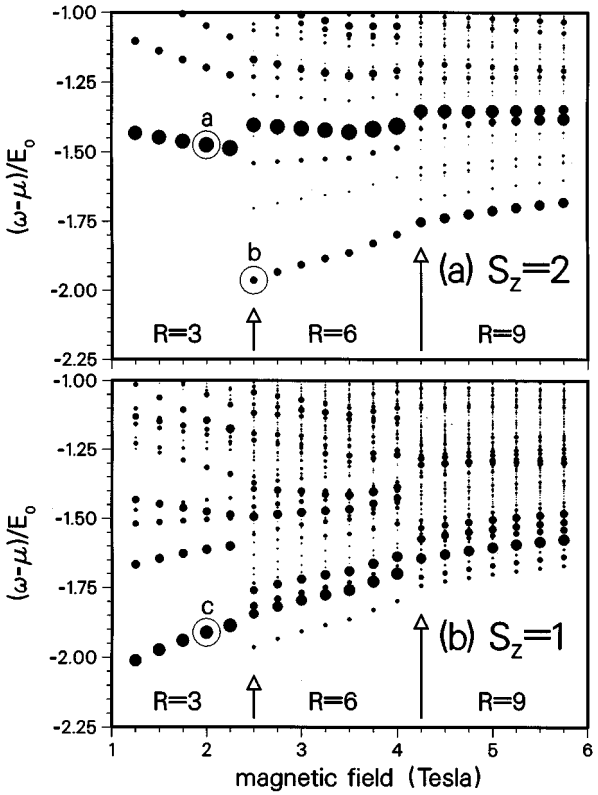

FIG. 6. Evolution of absorption spectra for three electrons ($3e\rightarrow 3e+X$) with increasing magnetic field. The areas of the black dots are proportional to the intensities of the peaks. Vertical arrows indicate magnetic-field-induced transitions in the initial three-electron system, between ''magic'' states with angular momenta $R=3$, 6, and 9. Two frames correspond to two different circular polarizations of the photon: (a) electrons in the final state are spin polarized and (b) a photoexcited electron has reversed spin. Occupation numbers of initial and final states for peaks marked with open circles (a)–(c) are shown in Fig. 7.

Since in the case of $S_z=1$ the photoexcited electron can be distinguished from three initial-state electrons due to opposite spin, we can observe in Fig. 7(c) a slight difference between the charge distributions of the photoexcited electron and a valence hole. This is a consequence of the fact that for the spin-unpolarized system, even at fixed charge distribution of the hole and all electrons (minimizing total kinetic energy and direct interaction energy), there is still the freedom to adjust the electronic spin distribution to maximize the attractive exchange interaction.

Around $B=2.5$ T the initial-state $N=3$ electron compact droplet breaks forming a ring with an empty hole in the center and consequently, for magnetic fields higher than 2.5 T, both polarizations of light may lead to the creation of an exciton occupying central low-energy orbitals. In the case of $S_z=2$ we hence observe the appearance of a new strong absorption peak at low energy [for $B=2.5$ T marked as *b*, the corresponding occupation-number graph in Fig. 7(b)], being a direct indication of the reconstruction of the dot. For $S_z=1$ the change in the spectrum is much less dramatic and now the lowest-energy peak corresponds to the electronic configuration with total spin $S=2$. Hence the difference in energies of the first peaks for both light polarizations is only

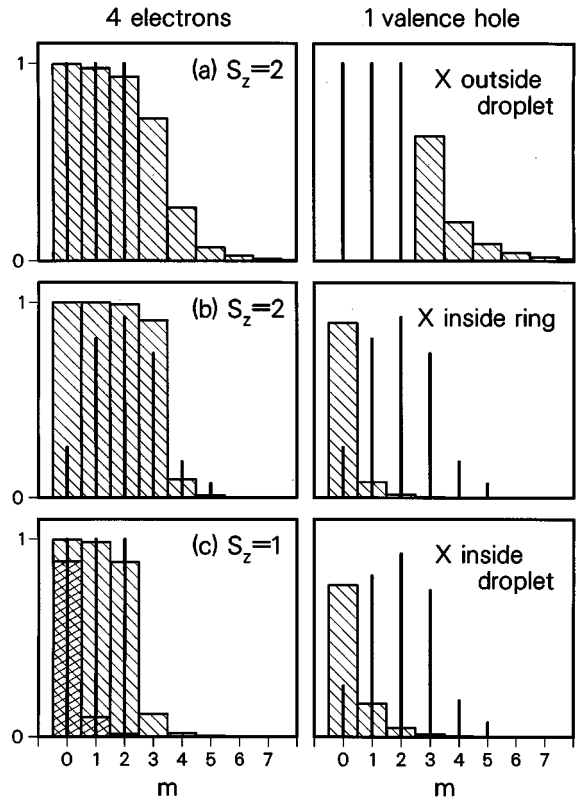

FIG. 7. Occupations of single-particle states $f(m)$ (approximately equal to the radial charge distribution) for initial $3e$ states (narrow black bars) and final $3e+X$ states (wide bars) in absorption for $N=3$. Corresponding peaks are marked with open circles in Fig. 6. (a) The initial three-electron state is compact and the exciton with the electron's spin down can be created only outside the droplet. (b) The initial state is a ring ($R=6$) and the exciton can be created in the center of the dot independently of spin. (c) The spin of photoexcited electron is reversed (different pattern of bars) and the exciton can be created inside the compact droplet.

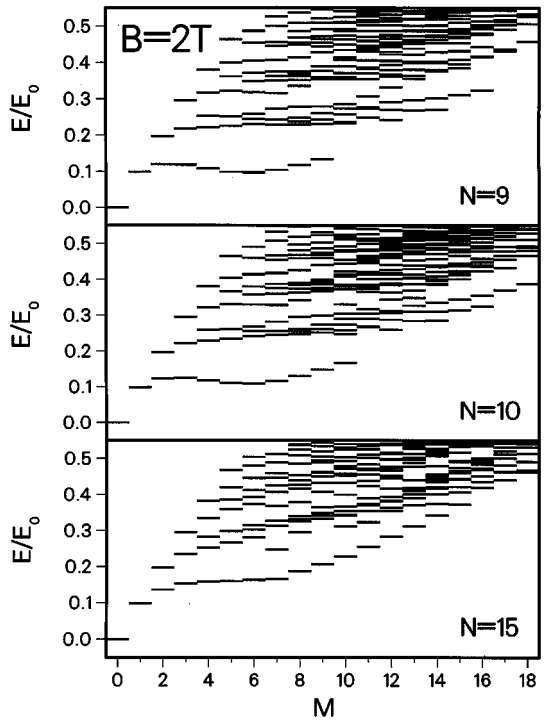

FIG. 8. Electronic excitation energies as a function of excess angular momentum M for $N=9$, 10, and 15 electrons at a magnetic field $B=2$ T. Corresponding filling factors for the ground states: $\nu=1$.

the small Zeeman shift. Both spectra shown in Fig. 6 are, however, still clearly distinguishable, as for $S_z=2$ there is a strong peak indicating the exciton created at the outer edge of the three-electron ring.

Comparing the charge distributions in the final and initial states for the transition corresponding to peak b [Fig.7(b)], we observe that not only the photoexcited electron fills the free space inside the $N=3$ electron ring, but additionally the hole attracts electrons closer to the center (*shakeup* effect). In consequence, the state of four compact electrons $|G_4\rangle$ and the hole occupying the $m=0$ orbital is a very good approximation of the actual state.

The next reconstruction of the three-electron ground state (from $R_A=6$ to 9) takes place around $B=4$ T. As seen in Fig. 6, the fairly small change in the absorption spectra reflects the fact that this reconstruction corresponds only to an expansion of the already existing $N=3$ electron ring due to the increasing strength of Coulomb repulsion and decreasing kinetic energy.

B. Excitons in a compact and reconstructed chiral Luttinger liquid

We now turn to larger dots. As an illustration of low-lying spectra for larger dots, the excitation spectra of electron droplets with $N=9$, 10, and 15 electrons in a magnetic field $B=2$ T are shown in Fig. 8. The first two spectra are the initial- and final-state excitation spectra in the absorption for the $N=9$ electron dot. The $N=15$ spectrum illustrates the lack of sensitivity of calculations to the number of particles.

The low-lying excitation spectra for $N=9,10,15$ show a well-developed maximum and minimum reminiscent of magnetorotons in the integer quantum Hall effect.[20] There is a single edge magnetoroton branch and a branch of bound magnetoroton pairs at higher angular momentum ($M\approx 10-18$) and energy.

To better understand the nature of the energy spectrum we show in Fig. 9 the full excitation spectrum, the one-pair excitation spectrum, and a two-pair excitation spectrum for $N=10$ electrons at $B=2$ T. The one-pair excitations form characteristic branches.[21] These branches can be labeled by the position of the excited electron. Hence the lowest branch is associated with excitations consisting primarily of an electron deposited at the outer edge of the dot and a hole traversing the interior of the dot. The two-pair excitation spectrum shows a minimum at $M=10$ characteristic of bound states.

The compact ($\nu=1$) ground state becomes unstable when the Coulomb energy begins to dominate the kinetic energy being optimized in the lowest angular momentum ground state. This transition manifests in soft modes, i.e., when the excitation energy becomes negative and ''magnetorotons'' condense to form a new ground state. The dot undergoes ''edge reconstruction'' at this point.

In Fig. 10 we show the energies for $N=15$ as a function of the magnetic field. With increasing B the magnetoroton

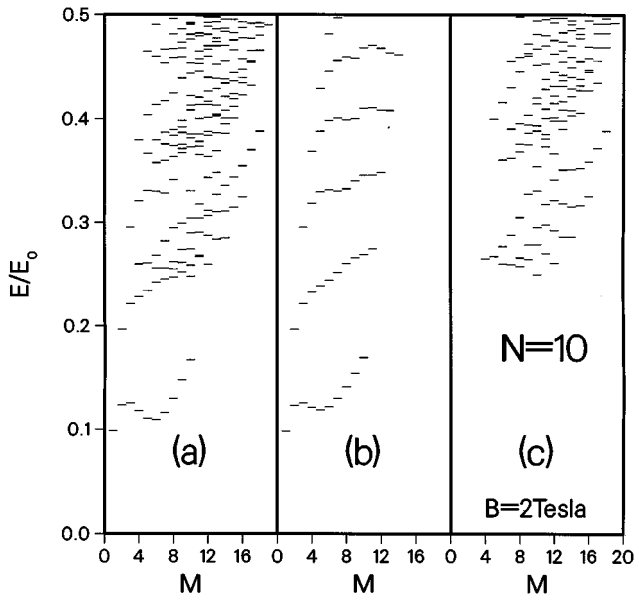

FIG. 9. Excitation spectra for 10 electrons at a magnetic field $B=2$ T: (a) total spectrum, with up to two-pair electron-hole excitations out of the compact droplet included; (b) one-pair excitations; and (c) two-pair excitations.

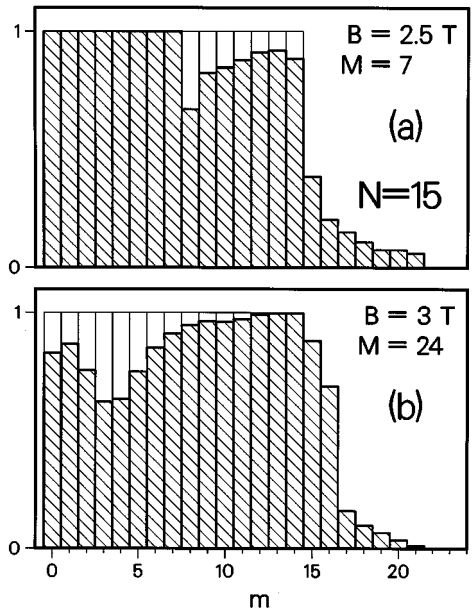

FIG. 11. Occupations of single-particle states $f(m)$ for the magnetoroton minima shown in Fig. 10: (a) first excited state at $B=2.5$ T, $M=7$; (b) ground state at $B=3$ T, $M=24$. Empty bars correspond to a compact state.

minimum develops in the excitation spectrum. In Fig. 11(a) we show the occupation of single particle states $f(m)=\langle c_m^\dagger c_m\rangle$ for the state $M=7$ corresponding to the magnetoroton minimum. The charge distribution corresponds to a hole penetrating the dot and an electron added to the outside of the dot. The correlated nature of this state is evident in the spreading of the charge of the hole and of the electron. Finally, when the magnetic field increases further, the lowest-energy state becomes either the one- or two-pair excited state.

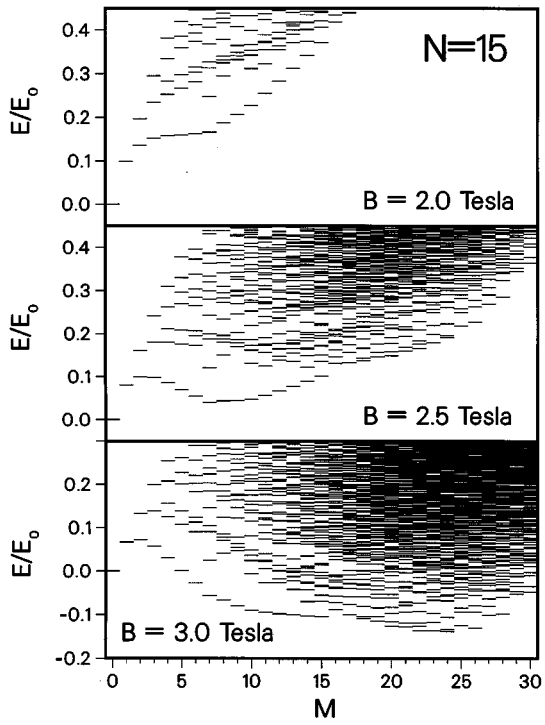

FIG. 10. Evolution of excitation spectrum for 15 electrons in an increasing magnetic field. At $B=2.5$ T there is a well-developed magnetoroton minimum at $M=7$. At $B=3$ T the ground state is the reconstructed state with $M=24$ (frozen magnetoroton).

In Fig. 10 we show the situation where the lowest-energy state is the two-pair excited state at $M=24$. The charge distribution $f(m)$ for this ''frozen'' magnetoroton state is shown in Fig. 11(b). It consists of holes spread in the center of the dot with electrons added to the edge of the dot. For a chiral Luttinger liquid, i.e., for the compact dot at $\nu=1$, we find a behavior that is not sensitive to particle number.

Examples of absorption spectra of a compact dot with $N=9$ electrons at $B=2$ T are shown in Fig. 12. In the absence of electron-hole interactions [$\alpha=0$, Fig. 12(a)], the absorption spectrum simply corresponds to a spectral function of a composite particle: edge magnetoroton and a valence-band hole. The energies correspond to the total energy of the complex while the oscillator strength reflects the particular way the electron is being added to the system. The first peak corresponds to adding an electron to the Fermi level, the second peak corresponds to adding an electron to the first excited state $M=1$. In both cases these are exact many-body states and have an oscillator strength of unity. When an electron is added further from the center of the dot, it becomes a part of the low-lying excitation of the $(N+1)$-electron dot: the edge magnetoroton. These excitations are here at energies comparable to the $M=1$ excitation. Hence the second peak ($M=1$) is broadened by edge magnetorotons, while at higher energies edge magnetoroton pairs contribute. The modulation of the density of states visible in the absorption spectrum is also illustrated by displaying a broadened absorption spectrum (solid line). The modulation

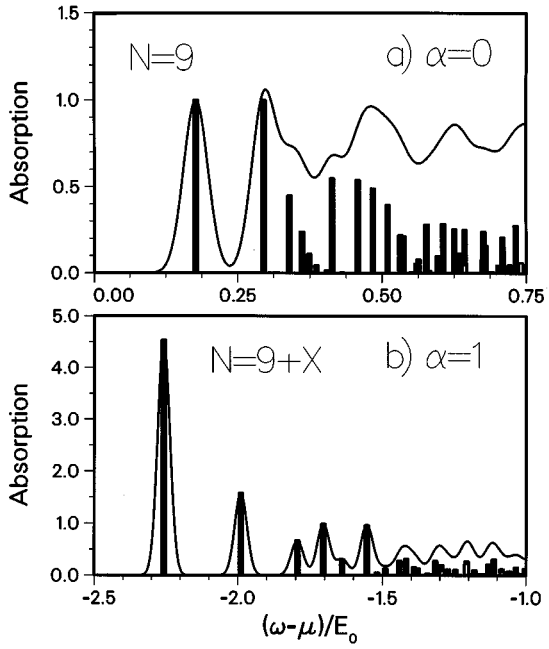

FIG. 12. Absorption spectra of a compact nine-electron dot at $B=2$ T (a) in the absence of electron-hole interactions $\alpha=0$ and (b) in the presence of electron-hole interactions $\alpha=1$. The case $\alpha=0$ corresponds to an electron spectral function, modified by the valence hole kinetic energy.

of the density of states is not significant in comparison to the density of states of the noninteracting system. This can be traced back to the small overlap of the excitation created by adding an electron away from the edge of the dot with edge magnetorotons. In edge magnetorotons an electron is always added to the edge of the droplet.

When the electron-hole interaction is switched on ($\alpha=1$), the oscillator strength of the lowest-energy transition growths, strongly resembling a Fermi edge singularity (FES). Of course, the FES discussed here is due to a large number of correlated many-electron states of the *interacting electron system* and not due to a change of noninteracting single-particle states induced by the attractive potential of the valence hole. In fact, in the absence of electron-electron interactions responsible for edge magnetorotons, there is no FES present here due to the gap in the single-particle excitation spectrum. The excitonic effects of course persist.

The shift of the transition reflects the renormalization of electron energies by the attractive valence-hole potential. The repulsive influence of an extra electron (magnetoexciton is charge neutral) is hidden in the chemical potential μ. The contribution of edge magneto-rotons appears as a shoulder at higher energies.

C. Recombination on acceptors in a compact droplet

We now illustrate the effects of interactions on the recombination with acceptors. The emission spectrum $E(\omega)$ for *a given position of acceptor* is given by summing all final states $|f\rangle$ with energies E_f according to Fermi's golden rule

$$E(\omega)=\sum_f \left|\left\langle f\left|\sum_{m=0}^{\infty} P_{0m}h_{0\uparrow}c_{m\downarrow}\right|i\right\rangle\right|^2 \delta(E_f+\omega-E_i). \tag{20}$$

Since the hole is tightly bound to the acceptor, the matrix elements P_{0m} do not depend strongly on the localized state $|0\rangle$ of the valence hole nor on the actual electron state $|m\rangle$, and we shall assume $P_{0m}=P_0=\text{const}$.

We also note that $h_{0\uparrow}c_{m\downarrow}|i\rangle=c_{m\downarrow}|G_{N+1}\rangle$ is the N-electron state with a well-defined total angular momentum $R=R_G^{N+1}-m$, where R_G^{N+1} is a fixed angular momentum of the initial $(N+1)$-electron state. Since the total angular momentum of final N-electron states $|f\rangle$ is a good quantum number, $E(\omega)$ is simply a spectral function of a hole (empty state) in the $(N+1)$-electron droplet with angular momentum m_f (m_f is the difference between the initial and final total angular momenta) created in the dot by the removal of an electron:

$$E(\omega)=P_0^2\sum_f |\langle f|c_{m_f\downarrow}|G_{N+1}\rangle|^2\delta(E_f+\omega-E_i). \tag{21}$$

This allows us to relate the emission spectrum to intrinsic electronic properties of a quantum dot.

Let us examine the recombination spectrum from a compact droplet. We express the creation of a hole in the $N+1$ compact droplet state $c_{m_f\downarrow}|G_{N+1}\rangle$ by the creation of an electron-hole pair excitation of the N-electron compact state $-c_{N\downarrow}^{\dagger}c_{m_f\downarrow}|G_N\rangle=|Nm_f\rangle$. The hole spectral function of an $(N+1)$-electron dot can be written in terms of the charge excitation spectrum of an N-electron dot:

$$E(\omega)=P_0^2\sum_f |\langle f|c_{N\downarrow}^{+}c_{m_f\downarrow}|G_N\rangle|^2\delta(E_f+\omega-\mu_N), \tag{22}$$

where E_f are the N-electron droplet excitation energies measured from the ground state and $\mu_N=E_i(N+1)-E_0(N)$ is the chemical potential of the N-electron dot. The final states $|f\rangle$ are expanded in one- and two-pair excitations and the Hamiltonian, including a repulsive acceptor potential, is diagonalized exactly in this basis. The matrix elements determine spectral weights. They involve an overlap of final states $|f\rangle$ with electron-hole pair excitation $|Nm_f\rangle$. This electron-hole pair excitation involves the removal of an electron from an occupied state in the bulk of the dot at $m=m_f$ and depositing it at the edge of the dot at $m=N$. These are simply states that contribute most to the low-lying excitations of the compact dot: edge magnetorotons. In Fig. 13 we show the excitation spectrum, at $B=2$ T, of the N-electron compact droplet in the absence of final-state interactions and the corresponding hole spectral function $E(\omega)$. The edge magnetorotons correspond to a group of states around $\omega\approx-0.1E_0$. The second group around $\omega\approx-0.24E_0$ corresponds to edge magnetoroton pairs. An important conclusion from this figure is that the hole spectral function has a very strong overlap with low-lying excitations of the compact dot. This is to be contrasted with the electron spectral function, which shows a very weak overlap with edge magnetorotons.

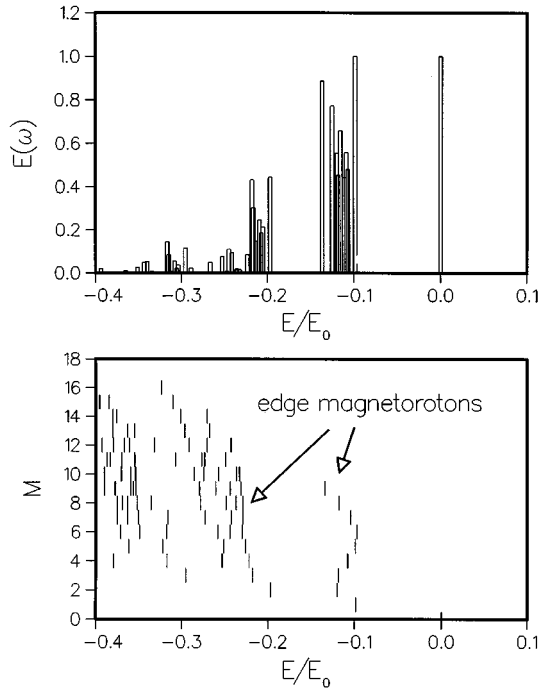

FIG. 13. Hole spectral function $E(\omega)$ and the excitation spectrum of a compact $N=10$ electron droplet.

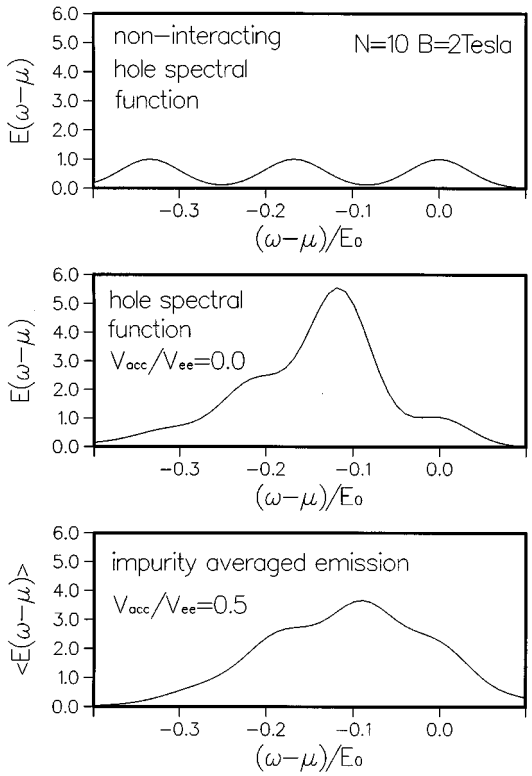

FIG. 14. Emission spectra of a compact $N=10$ electron droplet (a) without electron-electron interactions, (b) with electron-electron interactions but no finite state interactions, and (c) impurity averaged emission.

In Fig. 14 we show the recombination spectrum of (a) a noninteracting compact droplet; (b) an interacting compact droplet but without final-state interactions, i.e., no interaction with acceptor; and (c) an interacting compact droplet including the interaction with the acceptor in the final state, averaged over all possible acceptor positions within a single dot. The interaction of electrons with the acceptor was approximated by $\langle m|V_{\rm acc}|m\rangle=\delta\langle m,m_0|V_{ee}|m_0,m\rangle$, where $\delta=0.5$ measures the strength of the interaction and all acceptor positions $\langle\rho^2\rangle\approx m_0$ are equally probable. We see that the emission spectrum of the noninteracting system is drastically changed by electron-electron interactions. Instead of reflecting the zero-dimensional density of single-particle states, the spectrum is strongly enhanced at the Fermi energy (Fermi edge singularity) due to the emission of edge magnetorotons. This is a shakeup effect in this strongly correlated system. The shakeup appears to survive by averaging over different acceptor positions provided that the acceptors are sufficiently far away from the dot. The multiplet structure reflects edge magnetoroton pairs. The spectrum corresponding to an individual acceptor configuration of a small number of acceptors in a single dot could be observed using near field optical microscopy.

VI. CONCLUSION

In summary, a theory of strongly coupled magnetoexcitons and correlated electrons confined into quasi-two-dimensional parabolic quantum dots has been developed. The theory is readily applicable to, e.g., a wide class of self-assembled dots. Both electron- and valence-hole states have been treated in effective-mass approximation as Fock-Darwin states. The exact numerical calculations have been carried for the $N=3$ electron dot in strong magnetic fields. For a large number of electrons an expansion in one and two edge magnetoroton states was used to describe electron excitations, but the coupling with an exciton has been treated exactly.

In a strong magnetic field electrons form compact spin-polarized droplets. Increasing the magnetic field leads to transition between incompressible magic states of few-electron dots and a reconstruction of the edges of large dots. We show that these phenomena can be directly observed in interband absorption and emission in the form of additional peaks in the absorption spectrum.

The absorption-emission spectrum of compact (chiral Luttinger liquid) droplets shows an enhancement of the oscillator strength at the Fermi level. This enhancement is a manifestation of the Fermi edge singularity in strongly correlated and interacting electron systems. The Fermi edge singularity is accompanied by spectral features related to edge magnetorotons.

ACKNOWLEDGMENTS

This work was supported by NATO HTECH Grant No. 930746 and by the Institute for Microstructural Sciences, NRC Canada. J.A.B. was partially supported by RHAE-CNPq.

*Permanent address: Institute of Physics, Technical University of Wroclaw, Wybrzeze Wyspianskiego 27, 50-370 Wroclaw, Poland.

†Permanent address: Instituto de Fisica ''Gleb Wataghin''–DFESCM, Universidade Estadual de Campinas, 13081-970 Campinas, São Paulo, Brazil.

[1] For recent reviews and references see M. Kastner, Phys. Today **24** (1), 24 (1993); T. Chakraborty, Comments Condens. Matter Phys. **16**, 35 (1992).

[2] P. M. Petroff and S. P. Denbaars, Superlatt. Microstruct. **15**, 15 (1994).

[3] H. Drexler, D. Leonard, W. Hansen, J. P. Kotthaus, and P. M. Petroff, Phys. Rev. Lett. **73**, 2252 (1994).

[4] A. Wojs and P. Hawrylak, Phys. Rev. B **51**, 10 880 (1995).

[5] R. C. Ashoori, H. L. Stormer, J. S. Weiner, L. N. Pfeiffer, K. W. Baldwin, and K. W. West, Phys. Rev. Lett. **71**, 613 (1993); Bo Su, V. J. Goldman, and J. E. Cunningham, Science **255**, 313 (1992).

[6] P. Hawrylak, Phys. Rev. Lett. **71**, 3347 (1993).

[7] C. de Chamon and X.-G. Wen, Phys. Rev. B **49**, 8227 (1994); J. J. Palacios *et al.*, Europhys. Lett. **23**, 495 (1993); C. de Chamon *et al.*, Phys. Rev. B **51**, 2363 (1995).

[8] A. H. MacDonald, S. R. Eric Yang, and M. D. Johnson, Aust. J. Phys. **46**, 345 (1993).

[9] O. Klein *et al.*, Phys. Rev. Lett. **74**, 785 (1995).

[10] C. L. Kane, M. P. A. Fisher, and J. Polchinski, Phys. Rev. Lett. **72**, 4129 (1994).

[11] P. A. Maksym, Physica B **184**, 385 (1993); P. A. Maksym and T. Chakraborty, Phys. Rev. Lett. **65**, 108 (1990); Phys. Rev. B **45**, 1947 (1992).

[12] J. J. Palacios, L. Martin-Moreno, G. Chiappe, E. Louis, and C. Tejedor, Phys. Rev. B **50**, 5760 (1994); J. H. Oaknin *et al.*, Phys. Rev. Lett. **74**, 5120 (1995).

[13] V. M. Apalkov and E. I. Rashba, Solid State Commun. **93**, 193 (1995); X. M. Chen and J. J. Quinn, Phys. Rev. B **50**, 2354 (1994); A. H. MacDonald *et al.*, Phys. Rev. Lett. **68**, 1939 (1992); H. Buchmann *et al.*, *ibid.* **65**, 1056 (1990); A. J. Turberfield *et al.*, *ibid.* **65**, 637 (1990); B. B. Goldberg *et al.*, *ibid.* **65**, 641 (1990).

[14] P. Hawrylak, Phys. Rev. B **44**, 3821 (1991); T. Uneyama and L. J. Sham, Phys. Rev. Lett. **65**, 1048 (1990).

[15] P. Hawrylak and D. Pfannkuche, Phys. Rev. Lett. **70**, 485 (1993); D. Pfannkuche *et al.*, Solid State Electron. **37**, 1221 (1994).

[16] V. M. Apalkov and E. I. Rashba, Pis'ma Zh. Éksp. Teor. Fiz. **53**, 420 (1991) [JETP Lett. **53**, 442 (1991)].

[17] P. Hawrylak, Phys. Rev. B **45**, 4237 (1992); P. Hawrylak, N. Pulsford, and K. Ploog, *ibid.* **46**, 15 593 (1993); P. Hawrylak, Solid State Commun. **81**, 525 (1992).

[18] A. Petrou, M. C. Smith, C. H. Perry, J. M. Worlock, and R. L. Aggarwal, Solid State Commun. **52**, 93 (1984); I. V. Kukushkin, K. v. Klitzing, K. Ploog, and V. B. Timofeev, Phys. Rev. B **40**, 7788 (1990); A. S. Plaut, H. Lage, P. Grambow, D. Heitmann, K. von Klitzing, and K. Ploog, Phys. Rev. Lett. **67**, 1642 (1991); H. Buhmann, W. Joss, K. von Klitzing, I. V. Kukushkin, G. Martinez, A. S. Plaut, K. Ploog, and V. B. Timofeev, *ibid.* **65**, 1056 (1990); H. Buhmann, W. Joss, K. von Klitzing, I. V. Kukushkin, A. S. Plaut, G. Martinez, K. Ploog, and V. B. Timofeev, *ibid.* **66**, 926(1991); I. V. Kukushkin, N. J. Pulsford, K. von Klitzing, K. Ploog, R. J. Haug, S. Koch, and V. B. Timofeev, Phys. Rev. B **45**, 4532 (1992).

[19] M. D. Stone, H. W. Wyld, and R. L. Schult, Phys. Rev. B **45**, 14 156 (1992); M. D. Stone, Int. J. Mod. Phys. **5**, 503 (1990).

[20] C. Kallin and B. I. Halperin, Phys. Rev. B **31**, 3635 (1985); J.-W. Wu, P. Hawrylak, and J. J. Quinn, *ibid.* **31**, 6592 (1985).

[21] P. Hawrylak, Phys. Rev. B **51**, 17 708 (1995).